Available online at www.sciencedirect.com

ScienceDirect

Applied Ocean Research 00 (2021) 1–16

Journal Logo

Modelling and design of a perfectly-absorbing wave energy converter

R. Porter

School of Mathematics, Fry Building, Woodland Road, University of Bristol, Bristol, BS8 1UG, UK.

Abstract

This paper concerns the absorption of energy from two-dimensional water waves propagating over fluid of constant depth by a wave energy converter consisting of small buoyant floating rafts constrained to move in heave motion and attached to the bed with springs and dampers. Under a shallow water approximation to the fluid motion, it is shown that spatially-varying spring and damper settings allow all of the wave energy to be absorbed from all wave frequencies. The basis of the design is a formulation of a novel type of 'Perfectly Matched Layer' equation which can be mapped onto a shallow water model of the wave energy converter. The theoretical predictions are tested with computations based on a full description of linearised water waves and show that near-perfect absorption persists over a wide range of wave frequencies.

Keywords: Wave energy converter, perfectly matched layer, complete absorption.

1. Introduction

This paper concerns the absorption of energy from two-dimensional water waves incident on an array of buoys floating on the surface of a fluid. The question we concern ourselves with is whether it is possible to design the operation of these buoys to absorb all of the available incoming wave energy, not just at a single frequency but across wave frequencies. There is well-established theory (e.g. Evans (1976)) and multiple examples of two-dimensional ocean wave energy absorbers capable of extracting 100% of the wave energy, but only at particular wave frequencies. Examples include Salter's Duck (Salter (1974), Salter *et al.* (1976)) and the Bristol Cylinder (Evans *et al.* (1979)).

Our question will be addressed within the framework of linearised shallow water theory in which it is assumed the wavelength of propagating waves is significantly larger than the depth. Waves are incident from $x < 0$ over constant depth and the absorbing array of floating buoys extend into $x > 0$. The buoys are assumed to be much smaller in width than the wavelength and are connected to the bottom of the fluid by springs and dampers. The spring and damper

Email address: `richard.porter@bristol.ac.uk` (R. Porter)

settings are allowed to vary spatially along the device. We will show that it is possible under this framework to achieve perfect absorption across all frequencies.

The study in this paper is of more theoretical than practical interest. First, shallow water theory is an approximation for $kh \ll 1$ which is only exact (e.g. Porter (2019)) in the limit of $kh \to 0$ (k being the wavenumber, h the depth) and wave energy converters would be expected to operate in the regime $kh = O(1)$. Second, the perfectly-absorbing wave energy converter design extends indefinitely into $x > 0$ and requires a short initial segment of the array to contain negative dampers. On the other hand, the particular design being proposed within this paper does have some close relatives that have been considered as practical wave absorbers in the form of floating articulated rafts of the type originally conceived by Cockerell *et al.* (1978) and subsequently studied theoretically and numerically by Haren & Mei (1979) and Newman (1979). Significantly, the work of Haren & Mei (1979) was performed using shallow water assumptions and they carried out a comparison with numerical results for arbitrary depth suggesting that shallow water predictions performed well for larger fluid depths.

Compact arrays of floating buoys moving independently in heave as wave energy absorbers have been studied recently by Garnaud & Mei (2009) though not under shallow water theory. Garnaud & Mei (2009) use a multi-scale homogenisation method to develop an effective boundary condition to take account of the presence of the buoys based on their horizontal lengthscale being much smaller than that of the wavelength and their draft being insignificant. This careful approach is equivalent to invoking a continuum description of the surface loading similar to that proposed by Weitz & Keller (1950) and is how we choose to present the modelling here.

The paper contains two novel elements. The first is the development of a model of compact arrays of absorbing buoys under shallow water assumptions (see Section 4). This model has been derived in a physically intuitive manner although careful asymptotic analysis is needed to establish the correct matching conditions at the junction between the device and open water. The second is the development of a new family of equations which can be perfectly impedance matched at the boundary $x = 0$ between the unloaded and loaded surfaces and gives rise to wave decay in $x > 0$ (see Section 3.1). These ideas are related to the Perfectly Matched Layer (PML) equations originally due to Berenger (1994) which are explained, for context, in Section 3 of the paper. In Section 5 we consider the full linearised equations of water waves and produce numerical results to test the design of the proposed wave energy converter over a range of frequencies beyond $kh \ll 1$ and into $kh = O(1)$. We also assess the effect that the length of truncated devices have on absorption efficiency. The paper is summarised in Section 6.

2. Linearised shallow water equations

This short section provides an outline derivation of the linearised shallow water equation – see e.g. Stoker (1957) or Mei (1983) and references therein. It provides a platform for later discussion and model derivation.

Cartesian coordinates (x, z) are used with x lying horizontally in, and z upwards from, the mean free surface of a fluid of density ρ and constant depth h subject to gravity, g. The flow is two-dimensional with velocity $\mathbf{u} = U\hat{\mathbf{x}} + W\hat{\mathbf{z}}$ and support waves of height $\zeta(x, t)$. Shallow water assumes that the characteristic wavelength L is much greater than the depth and implies that

$U = U(x, t)$ and $W \ll U$ to leading order in h/L. Integrating $\nabla \cdot \mathbf{u} = 0$ with respect to z over the fluid depth, using the kinematic condition $\zeta_t = W$ on $z = \zeta$, gives

$$\zeta_t = -(h + \zeta)U_x \approx -hU_x \tag{1}$$

(i.e. equations are linearised supposing waves of sufficiently small amplitude). The z-component of the linearised Euler equations is approximately (i.e. neglecting W_t, a consequence of the shallow water assumption) $p_z = -\rho g$ and integrating, using $p = p_a$ (constant atmospheric pressure) on $z = \zeta$, gives

$$p = p_a + \rho g(\zeta - z). \tag{2}$$

The x-component of the linearised Euler equations is $\rho U_t = -p_x$ which then gives

$$U_t = -g\zeta_x \tag{3}$$

and combining equations to eliminate U gives

$$\zeta_{tt} = c^2\zeta_{xx} \tag{4}$$

where $c = \sqrt{gh}$.

3. Perfectly Matched Layers

Berenger's (1994) paper describes a method for absorbing waves at the boundary of truncated domains, designed for use in numerical methods aimed at providing computational solutions to solve Maxwell's equations. In his paper Berenger considered two-dimensional time-dependent problems associated with transverse electric/magnetic polarised waves and prescribed a non-physical set of partial differential equations (PDEs) which are perfectly impedance-matched to Maxwell's equations. These provide a reflectionless boundary across which obliquely-incident wave energy is perfectly transmitted and then progressively damped. Although the original method has been developed, generalised and adapted to other field theories, Berenger's original work considered Maxwell's equations under polarisation as coupled first-order PDEs for the electric and magnetic fields. The so-called Perfectly Matched Layer (PML) equations involve addition of damping to each equation in exactly the right balance to match the impedance to that of free space. For our purposes we consider how the PML works in a simpler one-dimensional setting and relating to waves on shallow water described, as already shown, by two field variables satisfying coupled first-order PDEs.

In $x < 0$ we take the shallow water equations (1), (3) or combined as (4). In $x > 0$ the PML is defined by the non-physical equations

$$U_t + c\lambda U = -g\zeta_x, \qquad \zeta_t + c\lambda\zeta = -hU_x \tag{5}$$

where λ is a positive constant, which may also be combined to give

$$\zeta_{tt} + 2c\lambda\zeta_t + c^2\lambda^2\zeta = c^2\zeta_{xx}. \tag{6}$$

The matching conditions at $x = 0$ are that ζ is continuous (a proxy for pressure) and U is continuous (mass flux). To see how the PML works we write $\zeta = \Re\{\eta(x)e^{-i\omega t}\}$, $U(x,t) = \Re\{u(x)e^{-i\omega t}\}$ so that the equations (4) and (6) in the frequency domain are

$$\eta''(x) + k^2\eta(x) = 0, \qquad x < 0 \tag{7}$$

where $k = \omega/c$ and

$$\eta''(x) + (k^2 + 2ik\lambda - \lambda^2)\eta(x) = 0, \qquad x > 0 \tag{8}$$

with the matching conditions in the frequency domain found to be

$$\eta(0^-) = \eta(0^+), \qquad \eta'(0^-) = \frac{k}{k + i\lambda}\eta'(0^+). \tag{9}$$

Solutions of (7) due to an incident wave from minus infinity are given by $\eta = e^{ikx} + Re^{-ikx}$ where R is the reflection coefficient whilst solutions of (8) are $\eta = Te^{i(k+i\lambda)x}$ with the transmission coefficient T associated with outgoing waves which decay as $x \to \infty$. The matching conditions (9) determine that $R = 0$ and $T = 1$. Since λ is a constant independent of frequency it follows that waves of all frequencies incident from $x < 0$ are absorbed without reflection by the PML equations (6) in $x > 0$.

It is hard to map the PML equations (5) onto a model of a physical system. Of particular difficulty is the conservation of mass equation which is modified in the second equation in (5) to include loss.

The PML of Berenger was modified and extended to a Generalised PML (GPML) by Fang & Zu (1995) to overcome some of the shortcomings of the PML, including its deficiency in suppressing evanescent waves. The downside of the GPML is that it is designed to operate for single frequency wave motion in which (5) become

$$(-i\omega + c\lambda(x))u = -g\eta', \qquad (-i\omega + c\lambda(x))\eta = -hu'. \tag{10}$$

In return, λ is no longer required to be constant and the two equations above combine to give

$$-\frac{\omega^2}{c^2}\eta = \frac{1}{1 + i\lambda(x)c/\omega}\left(\frac{\eta'}{1 + i\lambda(x)c/\omega}\right)'. \tag{11}$$

These equations result from what is sometimes referred to as 'coordinate stretching' of the undamped wave equation (4) via the complex mapping $x \to x + (ic/\omega)\int^x \lambda(s)\,ds$ and results in solutions in $x > 0$ of the form

$$\eta = T\exp\left\{ikx - \int^x \lambda(s)\,ds\right\}. \tag{12}$$

When λ is a constant we recover the Berenger PML, but this framework allows for the attenuation rate to increase smoothly which is important when implemented in discrete computational schemes like finite differences in suppressing numerically-induced reflections.

The time-domain PDE associated with (11), used in finite-difference time-domain numerical schemes, is

$$\frac{1}{c^2}\zeta_{tt} = \frac{1}{1 + \mathrm{i}\lambda(x)c/\omega}\frac{\partial}{\partial x}\left(\frac{1}{1 + \mathrm{i}\lambda(x)c/\omega}\frac{\partial \zeta}{\partial x}\right) \tag{13}$$

and, as already stated, there is an assumed frequency ω built into this PDE implying perfect absorption is tuned only to a particular frequency. There are extensions which incorporate frequency-independent PMLs but these add a significant degree of complication to the method which is not needed for the purposes of this paper.

3.1. A different approach

In $x < 0$ consider, as before, the one-dimensional frequency-domain wave equation

$$\eta''(x) + k^2\eta(x) = 0 \tag{14}$$

where $k > 0$ is constant and in $x > 0$ let η be governed by a general equation

$$\eta''(x) + \kappa(x)\eta(x) = 0 \tag{15}$$

and matching conditions at $x = 0$ are posed as

$$\eta(0^+) - \eta(0^-) = \beta\eta'(0^-), \qquad \eta'(0^+) = \alpha\eta'(0^-) \tag{16}$$

where α, β are constants. For the application we have in mind α, β will be real positive constants, independent of k, which puts our problem beyond the scope of the PML methods previously discussed.

We want to determine possible functions $\kappa(x)$ such that all incoming waves from $x = -\infty$ are absorbed in $x > 0$ and nothing is reflected by the boundary at $x = 0$.

In $x < 0$ the general solution of (14) is once again

$$\eta(x) = \mathrm{e}^{\mathrm{i}kx} + R\mathrm{e}^{-\mathrm{i}kx} \tag{17}$$

and so $\eta(0^-) = (1 + R)$ and $\eta'(0^-) = \mathrm{i}k(1 - R)$. In $x > 0$ we impose a solution of the form

$$\eta(x) = T\mathrm{e}^{\mathrm{i}Akx - f(x)} \tag{18}$$

where A is a positive real constant such that $f(0) = 0$ and $f(x)$ is a positive increasing function of x as $x \to \infty$ in order that $\eta(x) \to 0$ at infinity.

It follows that $\eta(0^+) = T$ and $\eta'(0^+) = (\mathrm{i}Ak - f'(0))T$ and application of the matching conditions (16) gives

$$T - R - 1 = \mathrm{i}k\beta(1 - R), \qquad (\mathrm{i}Ak - f'(0))T = \mathrm{i}k\alpha(1 - R). \tag{19}$$

Setting the reflection coefficient to zero, $R = 0$, gives $T = 1 + \mathrm{i}\beta k$ with

$$A = \frac{\alpha}{1 + \beta^2k^2}, \qquad f'(0) = \frac{-\beta k^2\alpha}{1 + \beta^2k^2}. \tag{20}$$

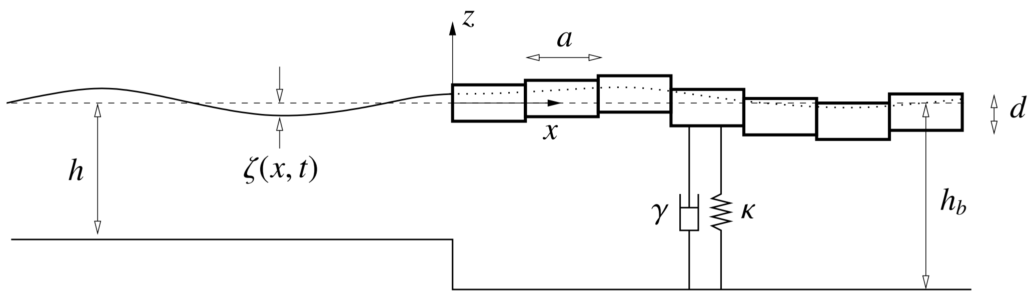

Figure 1. Sketch of the discrete floating absorbers and definition of the geometry.

as conditions on A and the function $f(x)$ for total absorption. From the definition (18) in $x > 0$

$$\eta'(x) = (\mathrm{i}Ak - f'(x))\eta(x) \tag{21}$$

and then

$$\eta''(x) = -f''(x)\eta(x) + (\mathrm{i}Ak - f'(x))^2\eta(x). \tag{22}$$

Comparison with (15) shows that

$$\kappa(x) = A^2k^2 + f''(x) - f'^2(x) + 2\mathrm{i}Akf'(x). \tag{23}$$

Note that if $\alpha = 1 + \mathrm{i}\lambda/k, \beta = 0$ and $f(x) = 0$ then we exactly recover the PML equations.

4. Shallow water model for an array of floating absorbers

Imagine that $x < 0$ an uncovered fluid is of constant depth h such that (4) holds and in $x > 0$ small buoyant rafts form a continuous cover of the surface of the fluid, each raft constrained to move in heave independently of its neighbours (see Fig. 1). The density of the buoys is $\rho_b < \rho$ and their depth is d so the draft of the buoys at rest is $\hat{\rho}d$ where $\hat{\rho} = \rho_b/\rho$. The width of the buoys, a say, is assumed to be much smaller than the wavelength and consequently the vertical displacement from equilibrium of the buoys due to the fluid motion may be described by a continuous function $\zeta(x, t)$ which satisfies the following dynamic equation

$$\rho_b d\zeta_{tt} = p|_{z=-\hat{\rho}d+\zeta} - p_a - \rho_b dg - \gamma\zeta_t - \sigma\zeta. \tag{24}$$

Each buoy is attached to a linear damper, γ, and a spring of spring constant σ (attributed values are per unit length). All terms in this equation can be varying slowly (on a lengthscale no smaller than that of the wavelength) with x under this continuum description of the buoys. This continuum description can be justified formally using multi-scale homogenisation similar to Garnaud & Mei (2009). Vertically integrating the continuity equation through the fluid $-h_b < z < -\hat{\rho}d + \zeta$ where h_b is the fluid depth under the buoys gives rise to

$$\zeta_t = -(h_b - \hat{\rho}d)U_x \tag{25}$$

after linearisation whilst vertical momentum integrates to $p = P(x, t) - \rho g z$ as before which, when used in (24) above, determines that

$$P(x, t) = \rho_b d\zeta_{tt} + p_a + \gamma\zeta_t + \sigma\zeta + \rho g\zeta. \tag{26}$$

Thus

$$p = p_a + \rho g(\zeta - z) + \rho_b d\zeta_{tt} + \gamma\zeta_t + \sigma\zeta \tag{27}$$

is the pressure in the fluid which, when used in horizontal momentum, $\rho U_t = -p_x$, gives

$$U_t = -g\zeta_x - \partial_x(\hat{\rho} d\zeta_{tt} + (\gamma/\rho)\zeta_t + (\sigma/\rho)\zeta). \tag{28}$$

Eliminating U between (25) and (28) results in the governing equation

$$\zeta_{tt} = (h_b - \hat{\rho} d)g\zeta_{xx} + (h_b - \hat{\rho} d)\partial_{xx}(\hat{\rho} d\zeta_{tt} + (\gamma/\rho)\zeta_t + (\sigma/\rho)\zeta) \tag{29}$$

under shallow water assumptions for wave propagation through floating buoys.

The matching conditions at $x = 0$ are that the pressure and mass flux are continuous. The second of these implies $hU(0^-, t) = (h_b - \hat{\rho} d)U(0^+, t)$ and results in

$$\frac{h}{h_b - \hat{\rho} d}\zeta_x(0^-, t) = \zeta_x(0^+, t) + \partial_x((\hat{\rho} d/g)\zeta_{tt} + (\gamma/\rho g)\zeta_t + (\sigma/\rho g)\zeta)|_{x=0^+}. \tag{30}$$

The first condition requires rather more careful attention. Shallow water theory is derived under the assumption that $\epsilon = kh = \omega\sqrt{h/g} \ll 1$ and subsequently expanding field variables in powers of ϵ. We have chosen to spare the reader that level of detail in order to preserve a more physical approach to the model derivation. However, we cannot completely ignore the consequences of a more formal approach which produce a boundary condition which is not physically intuitive. Thus, equations presented in this paper describing the fluid motion include contributions from zeroth and first order problems. In particular the damping term, which is associated with a time derivative, only enters the equations for the absorber in $x > 0$ at $O(\epsilon)$ and this is an effect which we are required to capture. We remark that expanding further to $O(\epsilon^2)$ is a far more serious undertaking (see Porter (2019)) and not one we need to entertain here. However, had it only been necessary to expand to zeroth order in ϵ then our matching condition would be that the pressure as $x \to 0^-$ matches the pressure as $x \to 0^+$ (this principle was applied to arrive at the first relation in (9)). The reason this is not an obvious condition to apply at higher orders is due to the abrupt change to the geometry at $x = 0$ in the levels of both the upper and lower fluid boundaries (see Fig. 1). This change to the vertical structure of the fluid implies that the shallow water models do not apply in the vicinity of $x = 0$. Formally, the matching across $x = 0$ from the solution in $x < 0$ to the solution in $x > 0$ must be performed by asymptotic matching to the solution of an inner problem with coordinates scaled to the depth, much smaller than the wavelength scale. This process contributes to the pressure matching condition at $O(\epsilon)$ and relating the pressure jump to the upstream flux multiplied by a "blockage coefficient" which depends only on the local geometry. This coefficient is found by solving a potential flow problem through the junction at $x = 0$ on which all lateral boundaries have Neumann conditions imposed and subject to unit upstream volume flux (see Appendix).

Such a process is described in excellent detail by Mei (1983), following Tuck (1975), for the problem of surface wave propagation over a step in the bed under shallow water conditions. In that work it is shown that changes in the modulus of the reflection coefficient due to the inclusion of a blockage coefficient appear at $O(\epsilon^2)$ which justifies their neglect. Here, unfortunately, the effect of the blockage coefficient cannot be so easily overlooked although its final effect is rather small.

Thus the difference in dynamic pressure equates to $-\rho(hU(0^-,t)[\psi])_t$ where $[\psi] = B$ is the potential difference and equal to the positive real blockage coefficient, B, multiplied by the upstream flux and is written, using (2), (27) as the condition

$$\rho g\zeta(0^+,t) + \rho_b d\zeta_{tt}(0^+,t) + \gamma\zeta_t(0^+,t) + \sigma\zeta(0^+,t) - \rho g\zeta(0^-,t) = -\rho BhU_t(0^-,t) \tag{31}$$

simplifying to

$$\zeta(0^+,t) + (\hat{\rho}d/g)\zeta_{tt}(0^+,t) + (\gamma/\rho g)\zeta_t(0^+,t) + (\sigma/\rho g)\zeta(0^+,t) - \zeta(0^-,t) = Bh\zeta_x(0^-,t) \tag{32}$$

after use of (3).

4.1. Frequency domain equations

In the case that waves of a single frequency, ω, are sought we write $\zeta(x,t) = \Re\{\eta(x)e^{-i\omega t}\}$ and $U(x,t) = \Re\{u(x)e^{-i\omega t}\}$ as before so that (4) becomes

$$\eta''(x) + k^2\eta(x) = 0, \qquad x < 0 \tag{33}$$

with $k = \omega/c$ and (29) is

$$\left(\left(1 - k^2\hat{\rho}dh - ik\frac{\gamma}{\rho}\sqrt{\frac{h}{g}} + \frac{\sigma}{\rho g}\right)\eta(x)\right)'' + \frac{k^2}{\hat{h}}\eta(x) = 0, \tag{34}$$

in $x > 0$ where $\hat{h} = (h_b - \hat{\rho}d)/h$. It helps to write $\hat{\sigma} = \sigma/\rho g$ and $\hat{\gamma} = \gamma/\rho\sqrt{gh}$ and, to be consistent with the derivation of the shallow water equation which implicitly neglect terms of order $O(kh)^2$, the equation above reads

$$((1 - ikh\hat{\gamma} + \hat{\sigma})\eta(x))'' + \frac{k^2}{\hat{h}}\eta(x) = 0. \tag{35}$$

We also make a change of variable

$$\tilde{\eta}(x) = (1 - ikh\hat{\gamma} + \hat{\sigma})\eta(x), \tag{36}$$

say, so that

$$\tilde{\eta}''(x) + \frac{k^2\tilde{\eta}(x)}{\hat{h}(1 - ikh\hat{\gamma} + \hat{\sigma})} = 0 \tag{37}$$

and recall that $\hat{\sigma}$ and $\hat{\gamma}$ can be functions of x varying on the lengthscale $O(1/k)$. It is straightforward to determine that the matching conditions (32), (30) have become, under both the transformations into the frequency domain and under the change of variable (36),

$$\tilde{\eta}(0^+) - \eta(0^-) = Bh\eta'(0^-) \tag{38}$$

and

$$\tilde{\eta}'(0^+) = \hat{h}^{-1}\eta'(0^-). \tag{39}$$

Using the shallow water assumption $kh \ll 1$ and, providing $\hat{\gamma} = O(1)$, we can approximate (37) by

$$\tilde{\eta}''(x) + \frac{k^2}{\hat{h}}\left(\frac{1}{1+\hat{\sigma}} + \mathrm{i}kh\frac{\hat{\gamma}}{(1+\hat{\sigma}^2)}\right)\tilde{\eta}(x) = 0 \tag{40}$$

a process equivalent to a formal asymptotic expansion of the governing equations to $O(kh)$. This governing equation with the matching conditions (38), (39) are aligned to the general system described in §3.1.

4.2. Perfect absorption

With reference to §3.1 we let $\alpha = \hat{h}^{-1}, \beta = Bh$ and it follows from (20) that

$$A = \frac{1}{\hat{h}(1+Bk^2h^2)} \approx \frac{1}{\hat{h}} \tag{41}$$

and

$$f'(0) = -\frac{Bk^2h}{\hat{h}(1+Bk^2h^2)} \approx -Bk^2h/\hat{h} \tag{42}$$

after ignoring $O(kh)^2$ to be consistent with the shallow water assumption. We are free to choose any $f(x)$ provided (42) holds, $f(0) = 0$ and $f(x)$ is positive increasing function of x as $x \to \infty$. We make the choice, for δ a positive constant,

$$f(x) = \frac{k^2h^2}{\delta}\ln\cosh(\delta x/h) - k^2hBx/\hat{h} \tag{43}$$

with $B/\hat{h} < 1$ and $f(x) \sim k^2h(1 - B/\hat{h})x$ as $x \to \infty$. In making the particular choice (43) we have been mindful of the consequences for the modelling assumptions, in particular that $\hat{\gamma} = O(1)$ and that spring constants should be positive. It follows that (15) holds with

$$\kappa(x) = \frac{k^2}{\hat{h}}\left[\frac{1}{\hat{h}} + \hat{h}\delta(1-\tanh^2(\delta x/h)) + \hat{h}k^2h^2(\tanh(\delta x/h) - B/\hat{h})^2 + 2\mathrm{i}kh(\tanh(\delta x/h) - B/\hat{h})\right]. \tag{44}$$

In view of wanting to align (44) with the coefficient in front of $\tilde{\eta}(x)$ in (40) we let $\hat{h}$ satisfy $\hat{h}^{-1}+\delta\hat{h} = 1$ to give

$$\hat{h} = (1 - \sqrt{1-4\delta})/(2\delta) \tag{45}$$

$(0 < \delta \le \frac{1}{4})$ and $\hat{h} \approx 1 + \delta$ for $\delta \ll 1$. Neglecting the $O(kh)^2$ term to be consistent with the shallow water equation derivation we can equate (44) to

$$\kappa(x) = \frac{k^2}{\hat{h}}\left(\frac{1}{1+\hat{\sigma}} + \mathrm{i}kh\frac{\hat{\gamma}}{(1+\hat{\sigma}^2)}\right) \tag{46}$$

with

$$\hat{\sigma}(x) = \frac{\delta\hat{h}\tanh^2(\delta x/h)}{1-\delta\hat{h}\tanh^2(\delta x/h)}, \qquad \hat{\gamma}(x) = \frac{2(\tanh(\delta x/h) - B/\hat{h})}{(1-\delta\hat{h}\tanh^2(\delta x/h))^2} \tag{47}$$

such that $\hat{\sigma}(x)$ increases monotonically from 0 at the origin to $\delta\hat{h}/(1-\delta\hat{h})$ at infinity. The damper settings are positive (absorbing) for $x > (h/\delta)\tanh^{-1}(B/\hat{h})$ and tend to the value $2(1-B/\hat{h})/(1-\delta\hat{h})^2$ as $x \to \infty$. However, for $0 < x < (h/\delta)\tanh^{-1}(B/\hat{h})$ the dampers are negative and consume energy to drive the device. The important feature of the springs and dampers in (47) is that they are independent of frequency and so this physical system absorbs all of the wave energy from all frequencies (albeit within the bounds of the model, namely shallow water).

The rate at which waves are damped is frequency dependent, since, for $kx \gg 1$

$$\eta \approx (1 + \mathrm{i}khB)\exp\{\mathrm{i}kx/\hat{h} - k^2h(1 - B/\hat{h})x\} \tag{48}$$

far into the array of absorbers, independent of the choice of δ. From a practical perspective, it would mean the array of floating absorbers would have to extend a distance in excess of $1/(k^2h)$ to get close to absorbing all of the available energy.

The value of B depends upon the local geometry – see the Appendix for the specification of the problem which determines B. If δ is small then $\hat{h} = 1 + \delta$ and the downstream fluid width is only marginally larger than upstream. If the draft of the buoys $\hat{\rho}d \ll h$ is small then the local junction in the geometry at $x = 0$ has little effect on the streaming flow and $B/\hat{h} \ll 1$. For example, for the shallow draft approximation given in (64) of the Appendix, $B/\hat{h} \approx -\delta^2\ln(\delta/2)/\pi$ for $\delta \ll 1$ and the length of the interval of the array which requires negative dampers is small relative to the depth: approximately $-\delta h\ln(\delta/2)/\pi$.

There may be other ways of representing wave attenuation through the buoy array with a choice of $f(x)$ different (43), which provide alternative solutions to the one proposed here.

5. Full linear theory

A question of immediate attention is whether the shallow water model developed in the previous section for the design of a perfect all-frequency wave energy converter extends beyond $kh \ll 1$ to $kh = O(1)$, a more practical range of frequencies. To answer this we must consider the full linearised equations for the small amplitude motion of a fluid with a free surface. In $x < 0$ where the surface is unloaded and the depth of the fluid is h, the fluid motion is governed by a velocity potential $\Phi(x,z,t)$ satisfying

$$\nabla^2\Phi = 0 \tag{49}$$

over $-h < z < 0$ with

$$g\Phi_z + \Phi_{tt} = 0, \quad \text{on } z = 0 \quad \text{and} \qquad \Phi_z = 0, \quad \text{on } z = -h. \tag{50}$$

In $x > 0$ the surface is covered with a compact array of independent heaving shallow-drafted floating buoys connected to springs and dampers over a bed of depth h_b. The governing Laplace equation (49) still holds for $-h_b < z < -\hat{\rho}d$ with $\Phi_z = 0$ on $z = -h_b$. On $z = -\hat{\rho}d$ the kinematic boundary condition is $\Phi_z = \zeta_t$ whilst the dynamic condition remains as (24), reliant on the continued assumption that the width, a, of each buoy is significantly smaller that the wavelength, but with the pressure in the fluid given by linearised Bernoulli's equation as

$$p = p_a - \rho\Phi_t - \rho g(-\hat{\rho d} + \zeta(x,t)). \tag{51}$$

The result of combining dynamic and kinematic conditions is

$$g\left(1+\frac{\hat{\rho}d}{g}\partial_{tt}+\frac{\gamma}{\rho g}\partial_t+\frac{\sigma}{\rho g}\right)\Phi_z+\Phi_{tt}=0, \qquad z=-\hat{\rho}d. \tag{52}$$

Writing $\Phi(x,z,t)=\Re\{\phi(x,z)\mathrm{e}^{-\mathrm{i}\omega t}\}$ implies $\nabla^2\phi=0$ in the fluid and $\phi_z=0$ on the bed of the fluid whilst from (50) and (51) we have

$$\phi_z-(\omega^2/g)\phi=0, \qquad z=0,\ x<0 \tag{53}$$

and

$$\phi_z-F(x)\phi=0, \qquad z=-\hat{\rho}d,\ x>0 \tag{54}$$

where

$$F(x)=\frac{(\omega^2/g)}{1-\omega^2\hat{\rho}d/g-\mathrm{i}(\omega\sqrt{h/g})\hat{\gamma}(x)+\hat{\sigma}(x)} \tag{55}$$

after using the same scalings on γ and σ introduced after (34).

This last boundary condition coincides with the one derived by Garnaud & Mei (2009) in a more general setting where buoys of circular cross section cover a fractional area of the surface, after taking into account the additional spring term. The total surface cover assumed here implies the inertia term proportional to ω^2 in the denominator, discarded at leading order by Garnaud & Mei (2009) on account of their scaling arguments, should be retained here. An independent study (by the current author, in preparation) confirms this. On the other hand the ratio of d/h is likely to be small and its effect is likely to be insignificant. Although Garnaud & Mei (2009) considered only constant damping, implicit in the multi-scale method used in the derivation of (52) is the capacity for the dampers $\hat{\gamma}$ and $\hat{\sigma}$ to vary on the lengthscale of the wavelength.

The task, therefore, is to design $\hat{\gamma}(x)$, $\hat{\sigma}(x)$ and select h_b to manufacture the same effect as in shallow water, namely total absorption of incoming wave energy over all frequencies. Evidently, the difficulty of this task is much increased here.

Instead, we take a different route and consider whether the perfect absorber design of $\hat{\gamma}(x)$, $\hat{\sigma}(x)$ made under shallow water conditions $kh \ll 1$ (equations (47)) work well for larger frequencies.

5.1. A 'mild slope' approach

Rather than attempt to solve the full linear equations directly we appeal to the fact that δ is small and the coefficient in surface condition (55) with (47) varies slowly with x/h. Because of this, we can use the approximation of Porter & Porter (2006) designed originally for solving two-dimensional wave scattering by significant changes in bathymetry. In that paper a conformal mapping of the domain with a variable fluid depth into a strip of uniform depth (e.g. Fitz-Gerald (1976), Roseau (1976)) was made whereupon the bathymetric variations are projected into a variable coefficient in the transformed free surface condition exactly in the form of (54), the only difference being that $F(x)$ in (55) is complex-valued. Porter & Porter (2006) developed their approximation by using an equivalent variational formulation of the boundary-value problem in $x>0$ and sought approximations to ϕ which are modulated by a depth variation associated with the dominant propagating modes assuming the surface coefficient $F(x)$ is locally constant. The step approximation (see Evans & Linton (1994)) could also be applied here although the recent work of Porter (2020) has shown the equivalence of 'mild slope' methods and step approximations.

In $x < 0$, the application of Porter & Porter (2006) is trivial and gives rise to the ordinary differential equation

$$\eta''(x) + k^2\eta(x) = 0, \tag{56}$$

where k now satisfies $k \tanh kh = \omega^2/g$. Since the surface coefficient is constant in $x < 0$ the propagating modes determined by solutions of (56) are exact.

In $x > 0$ the application of the mild slope method results in

$$\eta''(x) + \tilde{k}^2(x)\eta(x) = 0 \tag{57}$$

where $\tilde{k}(x)\tanh(\tilde{k}(x)(h_b - \hat{\rho}d)) = F(x)$. Note that (57) results from a simplification made by Porter & Porter (2006) which neglects a complicated modification to $\tilde{k}$ on the basis of it having a small effect – for our case the neglected terms are $O(\delta^2)$. The matching conditions are, as before, that

$$\eta(0^+) = \eta(0^-), \qquad \eta'(0^+) = \hat{h}^{-1}\eta'(0^-). \tag{58}$$

These matching relations arise on account of the variational principle used in Porter & Porter (2006). It can also be easily verified that the shallow water limit of this mild slope system coincides with the shallow water model (though only with $B = 0$), in particular $\tilde{k}^2(x) \to \kappa(x)$ in (46).

Solutions of (56) are $\eta(x) = \mathrm{e}^{\mathrm{i}kx} + R\mathrm{e}^{-\mathrm{i}kx}$ whilst solutions to (57) are determined by numerical integration. Specifically, we let

$$\eta(x) = C\eta_1(\hat{x}) + D\eta_2(\hat{x}) \tag{59}$$

where $\hat{x} = x/h$ and $\eta_i(x)$ are solutions to (57) in $x > 0$ set by the initial conditions $\eta_1(0) = 1$, $\eta_1'(x) = 0$ and $\eta_2(0) = 0$, $\eta_2'(x) = 1$. Since $\eta_i(\hat{x})$ will contain both exponentially decaying and growing solutions but we require $\eta(x) \to 0$ as $x \to \infty$ then from (59)

$$D = -C\eta_2(\hat{L})/\eta_1(\hat{L}) \tag{60}$$

where $\hat{L} = L/h \gg 1$ is a large numerical truncation parameter representing infinity. That is, large enough for the constant rate of exponential growth in the solutions to have established itself. From the behaviour predicted by (48) this should be in excess of $1/(kh)^2$. Numerically we have found the slightly odd choice $\hat{L} = 50/(kh)^{1.5}$ gives robust and accurate results for the particular numerical integration routine used (part of the NAG library). Matching the explicit solutions in $x < 0$ to (59) with (60) via (58) yields

$$R = \frac{\Lambda\eta_2(\hat{L}) - \eta_1(\hat{L})}{\Lambda\eta_2(\hat{L}) + \eta_1(\hat{L})}, \qquad \Lambda = \frac{-\mathrm{i}kh}{\hat{h}}. \tag{61}$$

where $\hat{h} = (h_b - \hat{\rho}d)/h$ as before. The same numerical solution can also be used to numerically approximate the proportion of incident wave energy absorbed by a device of finite length L. In $x > L$ we assume the depth returns to h and there exists a transmitted wave $\eta = T\mathrm{e}^{\mathrm{i}kx}$ propagating to infinity. For this case the reflection and transmission coefficients are easily found to be solutions of

$$\begin{pmatrix} \Lambda\eta_2(\hat{L}) + \eta_1(\hat{L}) & -1 \\ \Lambda\eta_2'(\hat{L}) + \eta_1'(\hat{L}) & \Lambda \end{pmatrix} \begin{pmatrix} R \\ T \end{pmatrix} = \begin{pmatrix} \Lambda\eta_2(\hat{L}) - \eta_1(\hat{L}) \\ \Lambda\eta_2'(\hat{L}) - \eta_1'(\hat{L}) \end{pmatrix}. \tag{62}$$

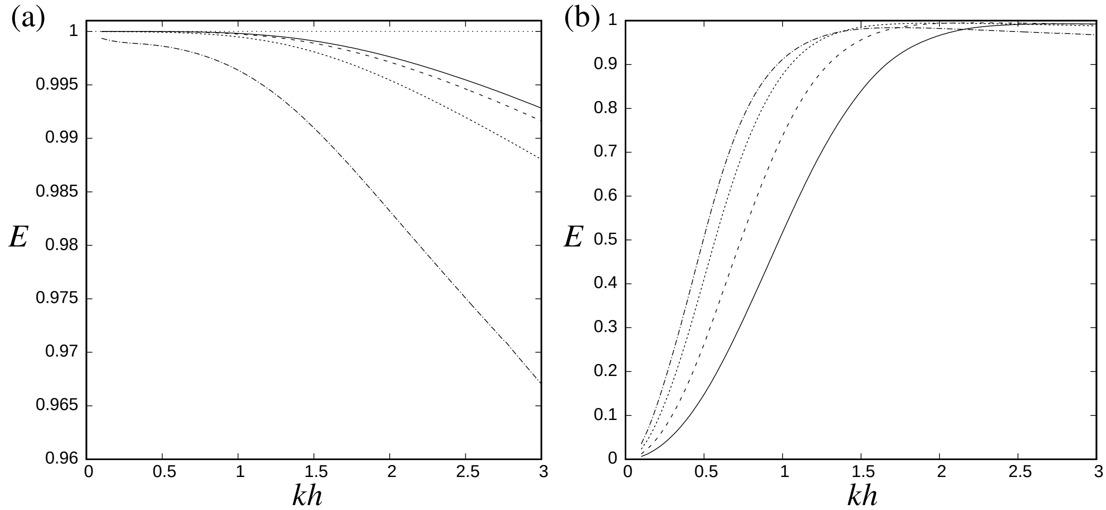

Figure 2. In (a) absorption efficiency against kh for $\delta = 0.025$ (solid), 0.05, 0.1, 0.2 (chained) for a device extending indefinitely into $x > 0$ and in (b) corresponding values for a device of finite length $\hat{L} = 5$.

5.2. Results

We are interested in the efficiency $E = 1 - |R|^2$ as a function of kh for the semi-infinite absorber and $E = 1 - |R|^2 - |T|^2$ for the absorber of dimensionless length $\hat{L} = L/h$. Perfect absorption implies $E = 1$.

We have taken $\hat{\rho} = 0.5$ and $d/h = 0.1$ as representative values in the computation of results using the mild slope approach described in the previous section. In Fig. 2 we show the variation of E against kh for values of δ between 0.025 and 0.2 assuming an absorber extending indefinitely into $x > 0$. As $kh \to 0$, $E \to 1$ since it is this limit where shallow water theory becomes exact. It can be seen that the efficiency remains remarkably high across a wide range of wavenumbers with smaller values of δ – implying a more gradual spatial variation of springs and dampers – giving the best results.

Numerical results have also been produced for an absorber in $x > 0$ with fixed values of $\hat{\gamma}(x) = 2/(1 - \delta\hat{h})^2$ and $\hat{\sigma}(x) = \delta\hat{h}/(1 - \delta\hat{h})$ and $h = h_b$ implying a sudden jump at $x = 0$ to the asymptotic values of spring and damper settings taken from the perfectly-absorbing design and with no adjustment of the depth. We have not displayed these results on any of the figures. However, we can report that $E \to 1$ as $kh \to 0$ though not asymptotically in the manner shown in Fig. 2(a); instead curves fall rapidly as kh increases to values around $E \approx 0.6$ when $kh = 3$ for all values of δ used in the figures. Thus, we assert that the performance of the perfectly-absorbing design is a significant improvement upon non-optimised designs having constant spring and damper settings.

In Fig. 3 we hold $\delta = 0.1$ constant and vary the length of the device from $\hat{L} = 2$ up to 16, confirming that longer devices lead to higher absorption from longer wavelengths.

The reader should be reminded that we never set out to optimise the performance of a wave absorbing device of finite length under $O(kh) = 1$ conditions. Having said that, it is interesting to note that there are similarities between the curves of efficiency produced here for devices of finite

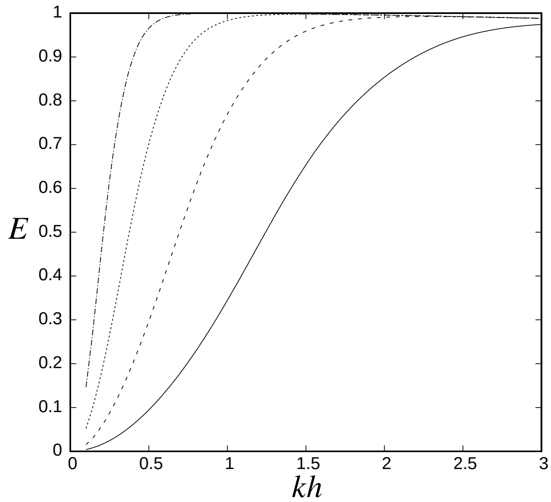

Figure 3. Absorption efficiency against kh for $\delta = 0.1$ and $\hat{L} = 2$ (solid), 4, 8, 16 (chained).

length and curves presented in Haren & Mei (1979) for optimally-designed articulated rafts.

6. Conclusions

We have developed a shallow water model of an array of floating buoys covering the surface to show that all of the energy incident in two-dimensional water waves can be absorbed from waves of all frequencies using spatially-varying spring and damper settings whose tuning is independent of frequency. The approach has relied on what is believed to be a novel variation of the Perfectly Matched Layer (PML) method of Berenger (1994) to perfectly impedance match the shallow water equations for an unloaded free surface to a loaded damped surface.

However, shallow water theory is an approximation for wavenumbers satisfying $kh \ll 1$ where h is the depth and is only exact in the limit $kh \to 0$. In addition to the proposed wave absorber being semi-infinite in extent implies that the main result is of more theoretical than practical interest.

On the other hand, we have also produced numerical results based on full linear theory to illustrate that perfect absorber design made under shallow water conditions can still absorb most of the available incident energy across a range of wavenumbers.

Appendix: The blockage coefficient

We solve the following problem for a potential $\psi(x,z)$ governed by $\nabla^2\psi = 0$ in the fluid domain $\{-\infty < x < 0,\ -1 < z < 0\} \cup \{0 < x < \infty,\ -h_b/h < z < -\hat{\rho}d/h\}$ with Neumann conditions all boundaries apart from those cutting the flow at the two infinities. As $x \to -\infty$ we impose $\psi(x,z) \to x$ and as $x \to \infty$ we have

$$\psi(x,z) = x/\hat{h} + B \tag{63}$$

where $\hat{h} = (h_b - \hat{\rho}d)/h$. The solution to this problem determines B. The problem is well suited to Schwarz-Christoffel mapping although the boundary in this problem is complicated and we have

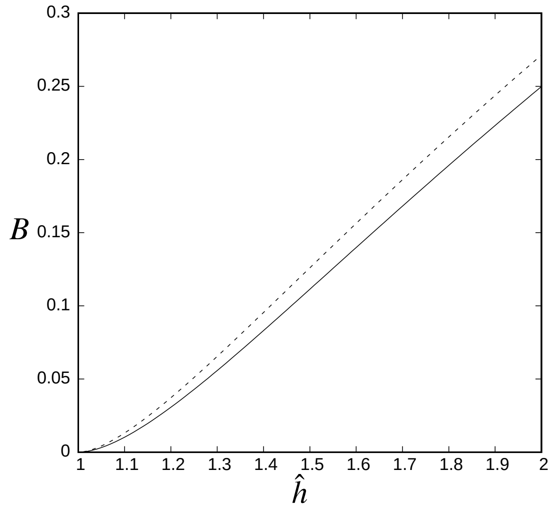

Figure 4. The variation of the blockage coefficient against $\hat{h}$ for $d/h = 0$ using the exact formula (solid) and the crude series approximation (dashed).

not attempted to calculate an explicit solution. In the case that $-\hat{\rho}d \approx 0$ the geometry is simplified and we have from Mei (1983),

$$B = \frac{1}{\pi}\frac{\hat{h}^2+1}{\hat{h}}\ln\left(\frac{\hat{h}+1}{\hat{h}-1}\right) - \frac{2}{\pi}\ln\left(\frac{4\hat{h}}{\hat{h}^2-1}\right) \approx \frac{-(\hat{h}-1)^2}{\pi}\ln((\hat{h}-1)/2) \tag{64}$$

for $\hat{h} \to 1^+$.

Alternatively, using separation solutions and mode matching to produce an integral equation for the horizontal flow velocity across $x = 0$ we can easily produce a crude but simple approximation to B which is

$$B \approx \frac{2}{\pi^3(1-\hat{\rho}d/h)^2}\sum_{n=1}^{\infty}\left\{\frac{\sin^2(n\pi\hat{\rho}d/h)}{n^3} + \frac{\hat{h}^2\sin^2(n\pi(1-\hat{\rho}d/h)/\hat{h})}{n^3}\right\} \tag{65}$$

which will work well for $\hat{\rho}d/h \ll 1$ and $h_b/h \ll 1$. A demonstration is provided by Fig. 4.

References

[1] Berenger, J.-P. A Perfectly Matched Layer for the absorption of electromagnetic waves. J. Comp. Phys. 1994:114;185-200.

[2] Cockerell, C., Platts, M. & Comyns-Carr, R. The development of the wavecontouring raft. In: Proc. Wave Energy Conference. London-Heathrow, H.M.S.O. London, Ed. P. Quarrell. 1978.

[3] Evans, D.V. A theory for wave-power absorption by oscillating bodies. J. Fluid Mech. 1976:77;1-25.

[4] Evans, D.V., Jeffrey, D.C., Salter, S.H. & Taylor, J.R.M. Submerged cylinder wave-energy device: theory and experiment. Appl. Ocean Res. 1979:1;3-12.

[5] Evans D.V. & Linton, C.M. On step approximations for water wave problems. J. Fluid Mech. 1994:278;229-249.

[6] Fang, J. & Wu, Z. Generalised Perfectly Matched Layer – An extension of Berenger's Perfectly Matched Layer boundary condition. IEEE Microwave & Guided Wave Lett. 1995:5(12);451-453.

[7] Fitz-Gerald, G.F. The reflexion of plane gravity waves travelling in water of variable depth. Phil. Trans. R. Soc. Lond. A. 1976:34;49-89.
[8] Haren, P. & Mei, C.C. Wave power extraction by a train of rafts: hydrodynamic theory and optimum design. Appl. Ocean Res. 1979:1(3);147-157.
[9] Garnaud, X. & Mei, C.C. Wave-power extraction by a compact array of buoys. J. Fluid Mech. 2009:635;389-413.
[10] Mei, C.C. The Applied Dynamics of Ocean Surface Waves. Wiley Interscience: New York. 1983.
[11] Newman, J. Absorption of wave energy by elongated bodies. Appl. Ocean Res. 1979:1(4);189–196.
[12] Porter, R. An extended linear shallow water equation. J. Fluid Mech. 2019:876;413-427.
[13] Porter, R. On the connection between step approximations and depth-averaged models for wave scattering by variable bathymetry. Q. J. Mech. Appl. Math. 2020:73(1);84-100.
[14] Porter, R. & Porter, D. Approximations to water wave scattering by steep topography. J. Fluid Mech. 2006:562;279-302.
[15] Roseau, M. Asymptotic Wave Theory. North-Holland. 1976.
[16] Salter, S.H. Wave power. Nature, 1974:249;720-724.
[17] Salter, S., Jeffery, D. & Taylor, J. The architecture of nodding duck wave power generators. The Naval Architect 1976:1;21-24.
[18] Stoker, J.J. Water Waves. Interscience, New York. 1957.
[19] Tuck, E.O. Matching problems involving flow through small holes. In Advances in Applied Mechanics, 1975:15;89-158.
[20] Weitz, M. & Keller, J.B. Reflection of water waves from floating ice in water of finite depth. Commun. Pure Appl. Maths 1950:3;581-607.